A Research Note on the Implementation of Star Formation and Stellar Feedback in Semi-Analytic Models

Fabio Fontanot[1], Gabriella De Lucia[2], Andrew J. Benson[3], Pierluigi Monaco[4], and Michael Boylan-Kolchin[5]

[1]*HITS-Heidelberger Institut für Theoretische Studien, Schloss-Wolfsbrunnenweg 35, 69118, Heidelberg, Germany*
[1]*Institut für Theoretische Physik der Universität Heidelberg, Philosophenweg, 16, 69120, Heidelberg, Germany*
[2]*INAF-Osservatorio Astronomico di Trieste, Via Tiepolo 11, I-34143, Trieste, Italy*
[3]*Carnegie Observatories, 813 Santa Barbara Street, Pasadena, California, 91101 USA*
[4]*Dipartimento di Fisica, sez. Astronomia, Universitá di Trieste, via G.B. Tiepolo 11, I-34143, Trieste, Italy*
[5]*Center for Cosmology, Department of Physics and Astronomy, 4129 Reines Hall, University of California, Irvine, CA 92697, USA*

January 28, 2015

Abstract

We study the impact of star formation and stellar feedback prescriptions on galaxy properties predicted by means of "stripped-down" versions of independently developed semi-analytic models (SAMs). These include cooling, star formation, feedback from supernovae (SNe) and simplified prescriptions for galaxy merging, but no chemical evolution, disc instabilities or AGN feedback. We run these versions on identical samples of dark matter (DM) haloes extracted from high-resolution N-body simulations in order to perform both statistical analysis and object-by-object comparisons. We compare our results with previous work based on stripped-down versions of the same SAMs including only gas cooling, and show that all feedback models provide coherent modifications in the distribution of baryons between the various gas phases. In particular, we find that the predicted hot gas fractions are considerably increased by up to a factor of three, while the corresponding cold gas fractions are correspondingly decreased, and a significant amount of mass is ejected from the DM halo. Nonetheless, we also find relevant differences in the predicted properties of model galaxies among the three SAMs: these deviations are more relevant at mass scales comparable to that of our own Galaxy, and are reduced at larger masses, confirming the varying impact of stellar feedback at different mass scales. We also check the effect of enhanced star formation events (i.e. starbursts modes), defined in connection with galaxy mergers. We find that, in general, these episodes have a limited impact in the overall star formation histories of model galaxies, even in massive DM halos where merger-driven star formation has often been considered very important.

Keywords: *galaxies: formation - galaxies: evolution - galaxies:fundamental properties*
email: fabio.fontanot@h-its.org

1 Introduction

In order to understand the complex process of galaxy formation over the entire cosmic history of the Universe, many different physical processes need to be taken into account. These processes act on different scales and their interplay appears critical for an appropriate description of the chain of events leading to the build up of present-day galaxy population. However, our comprehension of the physical processes acting on the baryonic components of these haloes is still limited.

A number of theoretical methods have been introduced, trying to get a better understanding of galaxy formation and evolution: among these different methods semi-analytic models (hereafter SAMs - for a review, see e.g. Baugh 2006) of galaxy formation and evolution have become a widely used tool, thanks to their flexibility and (relatively) low computational costs. In these models, relevant physical processes are included by assuming empirically and/or theoretically motivated prescriptions, coupled through a set of differential equations that describe the mass and energy flows between the different galactic components (i.e. halo, bulge and disc) and baryonic phases (i.e. stars, hot and cold gas).

A number of competing models have been proposed, assuming different (but equally plausible) descriptions of the relevant processes. Although the analysis of discrepancies and similarities between predictions from independently developed SAMs has been the subject of a number of recent studies (see e.g. Fontanot et al. 2009, 2011; De Lucia et al. 2011 and discussions therein), the role played by the overall SAM "architecture" (i.e. the more technical details of the construction of the models, and the interplay of their different assumptions) has not been analysed in detail.

A first step in this direction was given in De Lucia et al. (2010, hereafter DL10). In this study, we used "stripped-down" versions of three independently developed SAMs including only gas cooling and galaxy mergers. The models were run on identical sets of merger trees extracted from N-body simulations, so as to remove any systematic effect due to the adopted description of the dark matter evolution. We found a reasonable level of agreement between predictions from the three models, for the physical processes considered. In particular, the agreement is very good at dark matter haloes (DMHs) scales comparable to those of our own Milky-Way (MW). In the other hand, for larger masses, corresponding to those of clusters at $z = 0$, we found significantly different results in the predicted amount of cold gas, largely due to the different assumptions for the hot gas distribution inside DMHs, and to different treatments of the "rapid cooling" regime.

In DL10, we also compared the different treatment for the dynamical evolution of substructures and galaxy mergers, based either on fitting formulae derived from numerical simulations or analytic models accounting for dynamical friction, tidal stripping and tidal shocks. We showed that these different assumptions result in significant differences in the timings of mergers, with important consequences for the formation and evolution of massive galaxies.

In this research note, we extend the analysis of DL10 to investigate the influence of different prescriptions adopted for the physical mechanisms of star formation and SN feedback in both "quiescent" and "starburst" modes, avoiding to consider other processes like metal evolution, AGN feedback and disc instabilities and using simplified treatment of galaxy mergings. We stress that, given our limited understanding of the physical processes considered, all the prescriptions we will discuss in the following are equally plausible, so our analysis is not aimed at identifying the "best" model for star formation and feedback. Rather, the our aim is to analyse the influence of different model ingredients (and of the various modelling that can be adopted for specific processes) on the predicted properties of galaxies and their redshift evolution. As in DL10, we run our models on the same sets of merger trees extracted from numerical simulations. Results from our previous study allow us to control residual differences due to a different model for gas cooling and galaxy mergers.

In this work we use stripped-down versions of the *Munich* model by De Lucia & Blaizot (2007), the GALACTICUS model of Benson (2012) as an extension of *Durham* model of Bower et al. (2006), and the MORGANA model of Monaco et al. (2007). In all models we implement radiative cooling of a gas with primordial composition, star formation and SN feedback in "quiescent" and "starburst" regimes, including models of "super-wind" ejection from the DM halos and later re-accretions, and simplified prescriptions for galaxy mergers. We do not modify the choice of parameter values with respect to the original calibrations: we do not then expect predictions from these

stripped-down versions to be in any way representative of real galaxies, since they miss some key physical processes by construction, namely AGN feedback, metal evolution and disc instabilities. On the other hand, some of the excluded physical mechanisms are known to have a strong impact on predicted galaxy properties: since each model fine-tuning is done on versions including these additional processes, they could mask or reduce any difference due to the processes considered here.

2 Models

In the following, we briefly review the merger trees used and describe the main ingredients of the semi-analytic models focusing on the physical processes considered. We refer the reader to the original papers for more detailed descriptions; the not-interested reader may skip directly to sec.3.

It is worth stressing, that we make no effort to reduce the differences between the "cooling only" realizations shown in DL10. This choice allows us to keep our predictions as close as possible to the original formulation of the three SAMs under investigation. However, we consider two different sets of predictions relative to the *Durham* model, by considering both an isothermal and a cored profile for the hot halo. This choice allows us to compare predictions of the fiducial *Durham* model with those of a model that gives results closer to those obtained using the fiducial cooling models in MORGANA and the *Munich* SAM. Moreover, in order to exclude differences due to merger times ($t_{\rm mrg}$) assigned to satellite galaxies, we focus on a "no-merger" realization assuming $t_{\rm mrg} = \infty$ for all satellites. We also consider "instantaneous merger" realizations ($t_{\rm mrg} = 0$), and we will comment on the predictions of these models whenever appropriate.

We choose the same Chabrier IMF for all models and we switch off metal production in our model realizations (i.e. primordial composition is assumed during the entire evolution of our model galaxies). As a check, we have rerun our realizations allowing metal enrichment: the results presented in Section 3 are modified in the expected direction (e.g., cooling rates are systematically increased), but our main conclusions remain valid.

2.1 The Simulations and Merger Trees

In this work we take advantage of merger trees extracted from two large, high-resolution cosmological simulations, namely the Millennium Simulation (MS hereafter, Springel et al. 2005) and the Millennium-II Simulation (MSII hereafter, Boylan-Kolchin et al. 2009). The MS follows $N = 2160^3$ particles of mass $8.6 \times 10^8 {\rm M}_\odot/{\rm h}$ within a comoving box of size $500 {\rm Mpc/h}$ on a side. The MS-II follows the evolution of the same number of particles in a volume that is 125 times smaller than for the MS ($100 {\rm Mpc/h}$ on a side), with a correspondingly smaller particle mass ($6.9 \times 10^6 {\rm M}_\odot/{\rm h}$). For both simulations, the cosmological model adopted is a Λ cold dark matter (CDM) with $\Omega_m = 0.25$, $\Omega_b = 0.045$, $h = 0.73$, $\Omega_\Lambda = 0.75$, $n = 1$, and $\sigma_8 = 0.9$. The Hubble constant is parametrised as $H_0 = 100\,{\rm h\,km/s/Mpc}$. Group catalogues were constructed using the standard friend-of-friend (FoF) algorithm, and each group was then processed using the algorithm SUBFIND (Springel et al., 2001) to identify self-bound substructures.

We then consider the FoF merger trees constructed as detailed in DL10, and the same two sets of trees considered there. A first sample (the "MW-like" sample) has been constructed by selecting from the MS-II 100 haloes with $log_{10}(M_{200}/M_\odot)$ between 11.5 and 12.5 at $z = 0$. Here, M_{200} is defined as the mass within a sphere of density 200 times the critical density of the Universe at the corresponding redshift. A second sample of 100 haloes was selected from the MS by taking haloes that have a number density of $10^{-5} {\rm h}^3 {\rm Mpc}^{-3}$ at $z \sim 2$, and that end up in massive groups/clusters at $z = 0$. The adopted number density has been chosen to be comparable to that of submillimetre galaxies at $z \sim 2$ (Chapman et al., 2004, see e.g.,). We thus refer to this sample as the "SCUBA-like" sample.

2.2 The *Munich* model

The stripped-down version of the *Munich* model used in this work is built upon the De Lucia & Blaizot (2007) implementation and uses prescriptions for the star formation and feedback that have been described in detail in Croton et al. (2006). Cold gas is associated only to the disc component of model galaxies, and both a "quiescent" and a "starburst" mode for star formation are con-

sidered. Cold gas surface densities higher than a given threshold $\Sigma_{\rm crit}$ are required for quiescent star formation to take place. This critical value may be expressed in terms of the galactocentric distance (R) and the virial velocity of the host halo ($V_{\rm vir}$, Kauffmann 1996):

$$\Sigma_{\rm crit} = 120 \times \frac{V_{\rm vir}/200\,kms^{-1}}{R/kpc} M_{\odot} pc^{-2}\,, \qquad (1)$$

which can be translated into a critical mass, assuming the cold gas is uniformly distributed over a disc with outer radius $r_{\rm disc}$. The disc scale length (r_s) is computed using results from the model by Mo et al. (1998), and the outer radius of the disc is assumed to be $r_{\rm disc} = 3 \times r_s$. The critical gas mass for quiescent star formation to take place is:

$$M_{\rm crit} = 3.8 \times 10^9 \frac{V_{\rm vir}}{200\,kms^{-1}} \frac{r_{\rm disc}}{10Kpc} M_{\odot}\,. \qquad (2)$$

The star formation rate (SFR hereafter) φ is then assumed to occur at the rate:

$$\varphi_{\rm mun} = \alpha_{\rm mun} \frac{M_{\rm cold} - M_{\rm crit}}{\tau^{\rm mun}_{\rm dyn,D}}\,, \qquad (3)$$

where the star formation efficiency is set to $\alpha_{\rm mun} = 0.07$, and $\tau^{\rm mun}_{\rm dyn,D} = r_{\rm disc}/V_{\rm vir}$ is the disc dynamical time. The adopted modelling leads to episodic star formation self-regulating to maintain a level close to that corresponding to the critical surface density.

In addition to the quiescent mode, the model also allows for a "collisional starburst" mode of star formation (Somerville et al., 2001), triggered by galaxy mergers. The amount of cold gas converted into stars through this mode depends on the baryonic (gas + stars) mass ratio of the merging objects. If it is larger than 0.3, the event is classified as a "major" merger, and all cold gas present in the two merging galaxies is converted into stars. In the case of a minor merger, the model assumes that only a fraction $f_{\rm brs}$ of all available cold gas is converted into stars:

$$f_{\rm brs} = e_{\rm brs} \left(\frac{M_1}{M_2}\right)^{a_{\rm brs}}\,, \qquad (4)$$

where M_1/M_2 represents the baryonic mass ratio ($M_2 > 3M_1$), and $a_{\rm brs} = 0.7$ and $b_{\rm brs} = 0.56$ have been chosen to provide a good fit to the numerical simulations of Cox et al. (2004). Mergers also involve mass transfer between the disc and bulge components of the remnant galaxy. A detailed description on how galaxy mergers affect galaxy morphology is presented in De Lucia et al. (2011) and Fontanot et al. (2011). For the purposes of this work we do not distinguish between bulge and disc components of model galaxies, and focus on their global properties.

As for stellar feedback, the *Munich* model links the amount of cold gas reheated by SNe ($\Delta M^{\rm mun}_{\rm rht}$) in a given time interval to the mass of stars formed in the same time-step ($\Delta M_{\rm sf}$):

$$\Delta M^{\rm mun}_{\rm rht} = \epsilon_{\rm rht} \Delta M_{\rm sf}\,, \qquad (5)$$

where $\epsilon_{\rm rht} = 3.5$. The energy released in the same time interval ($\Delta E_{\rm SN}$) can be written as:

$$\Delta E_{\rm SN} = 0.5 V^2_{\rm SN} \eta_{\rm SN} \Delta M_{\rm sf}\,, \qquad (6)$$

where $0.5V^2_{\rm SN}$ represents the mean energy in SNe ejecta per unit mass of stars formed ($V_{\rm SN} = 630 kms^{-1}$ based on standard SNe theory and a Chabrier IMF), and $\eta_{\rm SN} = 0.35$ parametrises its efficiency in reheating the disc cold gas.

Adding the reheated gas to the hot halo without changing its specific energy leads to the total thermal energy change ($\Delta E_{\rm hot}$):

$$\Delta E_{\rm hot} = 0.5 V^2_{\rm SN} \times \Delta M^{\rm mun}_{\rm rht}\,. \qquad (7)$$

It is then possible to define an excess energy $E_{\rm exc} = \Delta E_{\rm SN} - \Delta E_{\rm hot}$. If $E_{\rm exc} < 0$, all reheated gas is confined within the halo, otherwise a fraction $\Delta M^{\rm mun}_{\rm eje}$ of hot gas mass ($M_{\rm hot}$) is ejected from the parent halo through a "super-wind":

$$\Delta M^{\rm mun}_{\rm eje} = \frac{E_{\rm exc}}{E_{\rm hot}} M_{\rm hot} = \left(\eta_{\rm SN} \frac{V^2_{\rm SN}}{V^2_{\rm vir}} - \epsilon_{\rm rht}\right) \Delta M_{\rm sf}\,, \qquad (8)$$

where $E_{\rm hot} = 0.5 V^2_{\rm vir} M_{\rm hot}$ represents the total thermal energy of the hot gas. The ejected material may be reincorporated at later times as the parent DMH grows (De Lucia, Kauffmann & White, 2004):

$$\dot{M}^{\rm mun}_{\rm rei} = \eta^{\rm mun}_{\rm rei} \frac{M_{\rm eje}}{\tau_{\rm dyn,H}}\,, \qquad (9)$$

where $\eta_{\rm rei}^{\rm mun} = 0.5$ is a free parameter which controls the amount of reincorporation per halo dynamical time, $\tau_{\rm dyn,H} = R_{\rm vir}/V_{\rm vir}$ ($R_{\rm vir}$ being the virial radius of the parent halo).

2.3 GALACTICUS

In the SAM comparison we presented in DL10 we made use of a stripped-down version of the Bower et al. (2006) implementation of the *Durham* model. There we tested two versions of the *Durham* model, the difference lying in the assumptions made for the profile of the hot gas distribution: we defined a "standard" model with a β-profile (as used by Bower et al. 2006) and a "modified" version using an isothermal profile.

In this work, we take advantage of the new GALACTICUS code (Benson, 2012) to recreate the stripped-down versions of the *Durham* models of DL10. GALACTICUS is designed to be highly modular to facilitate the exploration of different descriptions of key physical ingredients. We set-up GALACTICUS to run with the same assumptions[1] regarding gas cooling and gas profiles as in the standard and modified versions of the *Durham* code used in DL10. In the following, we will refer to these realizations as GALACTICUS-CP (for the β or cored profile) and GALACTICUS-IP (for the isothermal profile). We explicitly check that the "cooling only" stripped down versions of GALACTICUS reproduce with good approximation the predictions of the "cooling only" *Durham* model presented in DL10. We then include the same treatment for star formation and stellar feedback as depicted in Cole et al. (2000) and Benson et al. (2003, see also Bower et al. 2006), in order to create an equivalent of the *Durham* model needed for our analysis. Note that both the GALACTICUS-CP and GALACTICUS-IP models differ significantly from the default model in the GALACTICUS toolkit.

Galaxy sizes play a key role in this model since they determine dynamical times and rotation speeds in discs and spheroids. Given the angular momentum of cooling gas, the radii of galactic discs are computed by solving for the equilibrium radius at which rotation supports them against gravity in the combined potential of disc, spheroid and NFW dark matter halo (including the effects of adiabatic contraction). When spheroids are formed through major mergers (see below) their radii are computed by assuming conservation of (internal plus orbital) energy. Full details are given in Cole et al. (2000).

Star formation is assumed to occur in galactic discs, their cold gas reservoirs being depleted at a rate determined by the star formation timescale $\tau_{\rm sf}^{\rm dur}$:

$$\varphi_{\rm dur} = M_{\rm cold}/\tau_{\rm sf}^{\rm dur}\,. \tag{10}$$

The star formation timescale is a function of the disc circular velocity $V_{\rm disc}^{\rm HR}$ taken at the half-mass radius $r_{\rm disc}^{\rm HR}$:

$$\tau_{\rm sf}^{\rm dur} = \alpha_{\rm dur}^{-1}\tau_{\rm dyn,D}^{\rm dur}\left(\frac{V_{\rm disc}^{\rm HR}}{200 kms^{-1}}\right)^{\beta_{\rm dur}}\,, \tag{11}$$

where $\tau_{\rm dyn,D}^{\rm dur} = r_{\rm disc}^{\rm HR}/V_{\rm disc}^{\rm HR}$ represents the dynamical time of the disc, while $\alpha_{\rm dur} = 0.0029$ and $\beta_{\rm dur} = -1.5$ are free parameters.

When two galaxies merge, the merger is deemed to be "major" if the less massive of the galaxies is at least 30% of the mass of the more massive galaxy. In such cases, the stars of both galaxies are redistributed into a spheroid. Major mergers always trigger a starburst. Minor mergers may also trigger a starburst if the gas fraction in the more massive galaxy exceeds 10%. In starbursts, the gas content of the merging galaxies is placed into the spheroid component of the merger remnant, where it proceeds to form stars on a timescale given by eq. 11 but with $\alpha_{\rm dur} = 0.5$, $\beta_{\rm dur} = 0$, and with a dynamical time and velocity computed for the spheroid, using the method described by Cole et al. (2000).

Stellar feedback is modelled by assuming that the rate at which cold gas is reheated ($\dot{M}_{\rm rht}^{\rm dur}$) is directly related to the SFR:

$$\dot{M}_{\rm rht}^{\rm dur} = \left(\frac{V_{\rm disc}^{\rm HR}}{V_{\rm hot}}\right)^{-\gamma}\varphi_{\rm dur}\,, \tag{12}$$

where $V_{\rm hot} = 485 kms^{-1}$ and $\gamma = 3.2$ are free parameters. The reheated gas is not instantaneously returned to the hot phase, but it is stored into a separated reservoir, $M_{\rm rsv}$. This material is then added back to the hot phase at a rate equal to:

[1] In the GALACTICUS realization used in this work, all other relevant assumptions, including the definition of formation times, DM profiles and concentrations, merger time calculation, galaxy size calculations, and major merger definitions are treated as in the original *Durham* model.

$$\dot{M}^{\rm dur}_{\rm rei} = \eta^{\rm dur}_{\rm rei} \frac{M_{\rm rsv}}{\tau_{\rm dyn,H}}\,, \tag{13}$$

where $\eta^{\rm mun}_{\rm rei} = 1.26$ and $\tau_{\rm dyn,H}$ is the dynamical time of the dark matter halo. It is worth noting that the reheated material in GALACTICUS behaves as the ejected material in the *Munich* model, i.e. as a separated gas phase, which does not take part in the exchange of energy and mass inside the parent DMH, and which is slowly reincorporated into the hot phase. For a sake of simplicity, in the following, we will then refer to this component as ejected material:

$$\dot{M}^{\rm dur}_{\rm eje} = \dot{M}^{\rm dur}_{\rm rht}\,. \tag{14}$$

2.4 MORGANA

The MOdel for the Rise of GAlaxies aNd Agns (MORGANA) was first presented in Monaco et al. (2007). The treatment of star formation and stellar feedback in this code follows the results of the multiphase model for the ISM by Monaco (2004). For the purposes of this work we consider the combination of parameter values adopted when using a Chabrier IMF (Lo Faro et al., 2009).

Discs are treated as "thin" systems: SN remnants blow out of the disc soon after they form and most of the SNe energy is injected into the halo hot gas, and only a few percent of SNe energy injected into the ISM. The star formation timescale is of the form:

$$\tau^{\rm mor}_{\rm sf,D} = 9.1 \left(\frac{\Sigma_{\rm cold,D}}{1 M_\odot pc^{-2}}\right)^{-0.73} \left(\frac{f_{\rm cold,D}}{0.1}\right)^{0.45} Gyr\,, \tag{15}$$

where $f_{\rm cold,D}$ represents the cold gas fraction (in the disc component). Gas re-heated by stellar feedback is ejected from the disc to the an external reservoir of baryons (i.e. the "halo" component) still bound to the host DM halo, at a "hot wind" rate $\dot{M}_{\rm hw}$ assumed to be equal to the star formation rate:

$$\dot{M}_{\rm hw,D} = \varphi_{\rm mor,D}\,. \tag{16}$$

A fraction $f_{\rm th,D} = 0.32$ of SN energy $E_{\rm SN}$ is carried away with this ejected material, so the contribution $E_{\rm hw}$ of the hot wind to the thermal energy of the hot halo gas is:

$$\dot{E}_{\rm hw,D} = f_{\rm th,D} E_{\rm SN} \frac{\varphi_{\rm mor,D}}{m_{\rm SN}}\,. \tag{17}$$

where $m_{\rm SN}$ represents the mass of newly formed stars per SN. A further energy contribution is added by assuming that one type Ia SN per year explodes each 10^{12} $M_\odot$ of stellar mass. This rather crude implementation of energy from SNe Ia does not influence much model results.

Cold gas flows into the bulge component either by mergers or by disc instabilities. Moreover, a fraction of the cooling flow is allowed to fall directly into the bulge. Star formation in bulges is assumed to take place in a "thick" regime, where SN energy is effectively trapped within the ISM. In this case, SFR is assumed to follow a Schmidt-Kennicutt relation, with a timescale:

$$\tau^{\rm mor}_{\rm sf,B} = 4 \times \left(\frac{\Sigma_{\rm cold,B}}{M_\odot pc^{-2}}\right)^{-0.4} Gyr\,. \tag{18}$$

The size of the starburst, necessary to compute the gas surface density, is estimated as follows. Gas is assumed to have no angular momentum, and thus to be supported by turbulence generated by SNe. Under very simple assumptions (Lo Faro et al., 2009), the velocity dispersion in this case can be written as:

$$\sigma_{\rm cold} = \sigma_0 \left(\frac{\tau^{\rm mor}_{\rm sf}}{Gyr}\right)^{-1/3}\,, \tag{19}$$

where $\sigma_0 = 60$ km s^{-1} is treated as a free parameter. It is then assumed that the size of the starburst region is such that $\sigma_{\rm cold}$ equates the rotation curve of the bulge, assumed to be flat (see Lo Faro et al. 2009 for details).

The rate at which hot gas is ejected from a bulge to the host halo is assumed to be:

$$\dot{M}_{\rm hw,B} = \begin{cases} \frac{\sqrt{V^2_{\rm hot} - V^2_B}}{V_{\rm hot}} \varphi_{\rm mor,B} & \text{if } V_B < V_{\rm hot} \\ 0 & \text{if } V_B \geq V_{\rm hot} \end{cases} \tag{20}$$

This is done to take into account the ability of the potential well of a massive bulge to keep hot gas confined; the parameter $V_{\rm hot}$ is chosen to be 300 km/s, corresponding to the typical thermal velocity of a $\sim 10^7$ K hot phase. The corresponding energy carried by the hot wind is:

$$\dot{E}_{\rm hw,B} = f_{\rm th,B} E_{\rm SN} \frac{\sqrt{V^2_{\rm hot} - V^2_B}}{V_{\rm hot}} \frac{\varphi_{\rm mor,B}}{m_{\rm SN}}\,, \tag{21}$$

where we use $f_{\rm th,B} = 0.1$ for the fraction of SN energy carried away.

A bulge also ejects cold gas into the halo, due to the same SN-driven turbulence that sets the starburst size (Eq. 19). This "cold wind" from the bulge to the halo component is assumed to occur at a rate:

$$\dot{M}_{\rm cw,B} = \frac{M_{\rm cold,B} P_{\rm ub} v_{\rm ub}}{R_B}\,, \qquad (22)$$

where R_B is the half-mass radius of the bulge, while $P_{\rm ub}$ and $v_{\rm ub}$ represent the probability that a cold cloud is unbound (i.e. it has a velocity larger than the escape velocity of the bulge V_B) and the average velocity of unbound clouds (both probabilities are computed assuming a Maxwellian distribution of velocities with rms $\sigma_{\rm cold}$).

The hot and cold halo gas components keep track of both the mass and the energy received respectively from hot winds from discs and bulges and from cold winds from bulges. The halo receives winds both from the central galaxy and from satellites. Whenever the gas phases of the halo component are too energetic to be bound to the DM halo, they are allowed to escape to the IGM as a galaxy "superwind". In particular, if the energy $E_{\rm hot,H}$ of the halo hot gas mass $M_{\rm hot,H}$ overtakes the virial energy $E_{\rm vir}$ by more than a factor $f_{\rm wind} = 2$, a superwind occurs at a rate:

$$\dot{M}^{\rm mor}_{\rm eje,H} = \left(1 - \frac{f_{\rm wind} E_{\rm vir}}{E_{\rm hot,H}}\right) \frac{c_s M_{\rm hot,H}}{R_{\rm vir}}\,, \qquad (23)$$

where c_s represents the sound velocity in the halo. A similar formula determines the ejection of cold superwinds:

$$\dot{M}^{\rm mor}_{\rm eje,C} = \left(1 - \frac{f_{\rm wind} V^2_{\rm disp}}{\sigma^2_H}\right) \frac{\sigma_H M_{\rm cold,H}}{R_{\rm vir}}\,. \qquad (24)$$

A fraction ($f_{\rm back} = 0.5$) of the mass ejected by the DM halo is later re-incorporated (i.e. added to infalling IGM), when the parent DM halo reaches an escape velocity larger than the (thermal or kinetic) velocity the gas had when it was ejected.

2.5 Comparison between the models

All three models considered relate the SFR in the disc component to the amount of cold gas there available, but make different assumptions for the timescale of conversion. In the *Munich* model, the star formation proceeds on a timescale directly proportional to the dynamical time of the disc, while in *Durham*-like models the timescale of star formation is rescaled with some power of the circular velocity of the disc. Finally, MORGANA assumes a star formation timescale consistent with the Schmidt law. The *Munich* model explicitly accounts for a critical mass threshold for star formation, while MORGANA and *Durham*-like models do not.

Besides a quiescent mode of star formation, both the *Munich* and GALACTICUS-CP models assume an enhanced star formation regime occurring during galaxy mergers, with a fraction of the total cold gas available being turned into stars in a very short timescale (that of the model integration). In MORGANA, cold gas is associated also to the bulge component. Because of the complete loss of angular momentum, gas in bulges is concentrated to very small sizes. Then the higher gas surface densities force the Schmidt-Kennicutt relation to give much higher SFRs and shorter star formation timescales than those corresponding to star formation in discs. In our reference runs, we explicitly exclude merger events and the enhanced SFR by setting $t_{\rm mrg} = \infty$. We will discuss the impact of the "starburst" mode on the predicted star formation histories by considering the predictions of the instantaneous-merger runs in section 3.2.

In MORGANA the amount of disc gas reheated via stellar feedback ($M_{\rm rht}$) equals the SFR (φ), while in the *Munich* model these two quantities are proportional, via the parameter $\epsilon_{\rm rht} > 1$. This implies that the amount of reheated gas per unit star formation is always larger in the *Munich* model than in MORGANA . A slightly different choice has been made in the GALACTICUS models, where the amount of reheated gas remains proportional to φ, but is additionally assumed to scale as a power of the disc velocity.

An important quantity in the balance of the baryonic content of each DMH is given by the amount of baryons ejected. In both *Durham*-like and *Munich* models, the fraction of ejected mass is directly proportional to the mass of stars formed in the same time interval, while in MORGANA the dependency of the ejection rate on stellar feedback is mediated via the estimate of the thermal (kinetic) energy of the hot (cold) gas halo phase. All models assume that this ejected material is reincorporated into

the halo at later times, with different assumptions for the reincorporation rates. In *Durham*-like and *Munich* models, this is modelled as a continuous process following the DMH growth, while in MORGANA only half of the material connected to each ejection event is re-acquired instantaneously when the DMH has grown enough to overcome its escape velocity.

Durham-like and *Munich* models employ a very similar scheme for modeling the ejected component. In both cases some of the feedback reheated material is excluded from the mass/energy flows between the cold and hot gas phases: but while this is only a fraction in the *Munich* model (the remaining being instantaneously added to the hot phase), all reheated material is considered in the *Durham*-like models. The same reincorporation scheme is assumed, but with a faster rate in the *Durham*-like models than in the *Munich* model.

In the following, we choose to avoid the complications arising form disc instabilities[2] by switching them off.

3 Results

3.1 Test cases

We start by considering the evolution of the different baryonic components in a few test cases. For consistency with DL10, we focus on the same 4 representative DMHs (their fig. 1 and 4). These have been chosen among the 100 MW-like and the 100 scuba-like (two for each sample) as representative of a quiet mass accretion histories and of a large number of merger events. In the following, whenever we refer to "central galaxy" for our DMHs, we will refer to the central galaxy of the main progenitor at the corresponding redshift. All other galaxies will be defined as "satellites". For the sake of simplicity, in this section we will show results only for the 2 haloes with quiet mass accretion histories. The other two haloes give consistent results, and are shown for completeness in appendix A.

[2] In particular, disc instabilities have no direct effect on the SFR predicted by the *Munich* model, since only enough stellar mass is removed from the disc to the bulge to restore stability. In the *Durham* model, at each instability event, the whole disc is destroyed and all its baryons are given to the spheroidal component, with any cold gas present assumed to undergo a starburst. In MORGANA a different choice has been made, by moving a well defined fraction of disc stars and cold gas to the bulge, where it forms stars on a $\tau^{\rm mor}_{\rm sf,B}$ timescale.

Figures 1 and 2 show the redshift evolution of the different baryonic components in the haloes considered: from top to bottom, we show the cold gas fraction associated with the central galaxy, the hot gas fraction in the halo, the *net cooling rate* ($\dot{m}_{\rm NCR}$; see below), the stellar mass of the central galaxy and the mass ejected from the DMH. In the three upper panels, we compare the predictions of the models including star formation and feedback (darker colours - solid lines) with previous results for the "only cooling" realizations considered in DL10 (lighter colours - long dashed lines).

We define $\dot{m}_{\rm NCR}$ as the net rate at which cold gas and stars are deposited into the galaxy:

$$\dot{m}_{\rm NCR} = \frac{M_{\rm cold}(t_2)+M_{\rm star}(t_2)}{t_2-t_1} - \frac{M_{\rm cold}(t_1)+M_{\rm star}(t_1)}{t_2-t_1},$$

where t_1 and t_2 are the cosmic epochs corresponding to two consecutive snapshots. The net cooling rate differs from the intrinsic cooling rate, since it takes into account both the effect of feedback in removing part of the cold gas from the system and the effect of star formation in locking some material in long lived stars. For the stripped-down SAM versions considered in DL10 these two quantities coincide by construction.

The inclusion of feedback from star formation has the net effect of reducing the amount of cold gas available in MW-haloes (figure 1, this holds also for instantaneous merger realizations) and increasing the hot gas fraction with respect to the "cooling only" runs. In the MW haloes, this increase is particularly relevant in the *Durham*-like models, that predicts higher hot gas fraction with respect to the other two models. This shows that the feedback scheme implemented in the *Durham*-like models is the most efficient (among those considered here) in reheating the cold gas in the haloes at these mass scales. The cold gas fraction associated with the central galaxy is characterized by a marked decline at lower redshift, and predictions from the three models considered are more different than in the "cooling only" realizations. In our models there are two competing effects able to deplete the cold gas reservoir: the formation of long lived stars and cold gas removal by stellar feedback. In order to disentangle these two effects we consider the evolution of the overall cold gas plus stars and still find a decrease with respect to the predictions of DL10 for the cold gas component. These findings show that the inclusion of a strong stel-

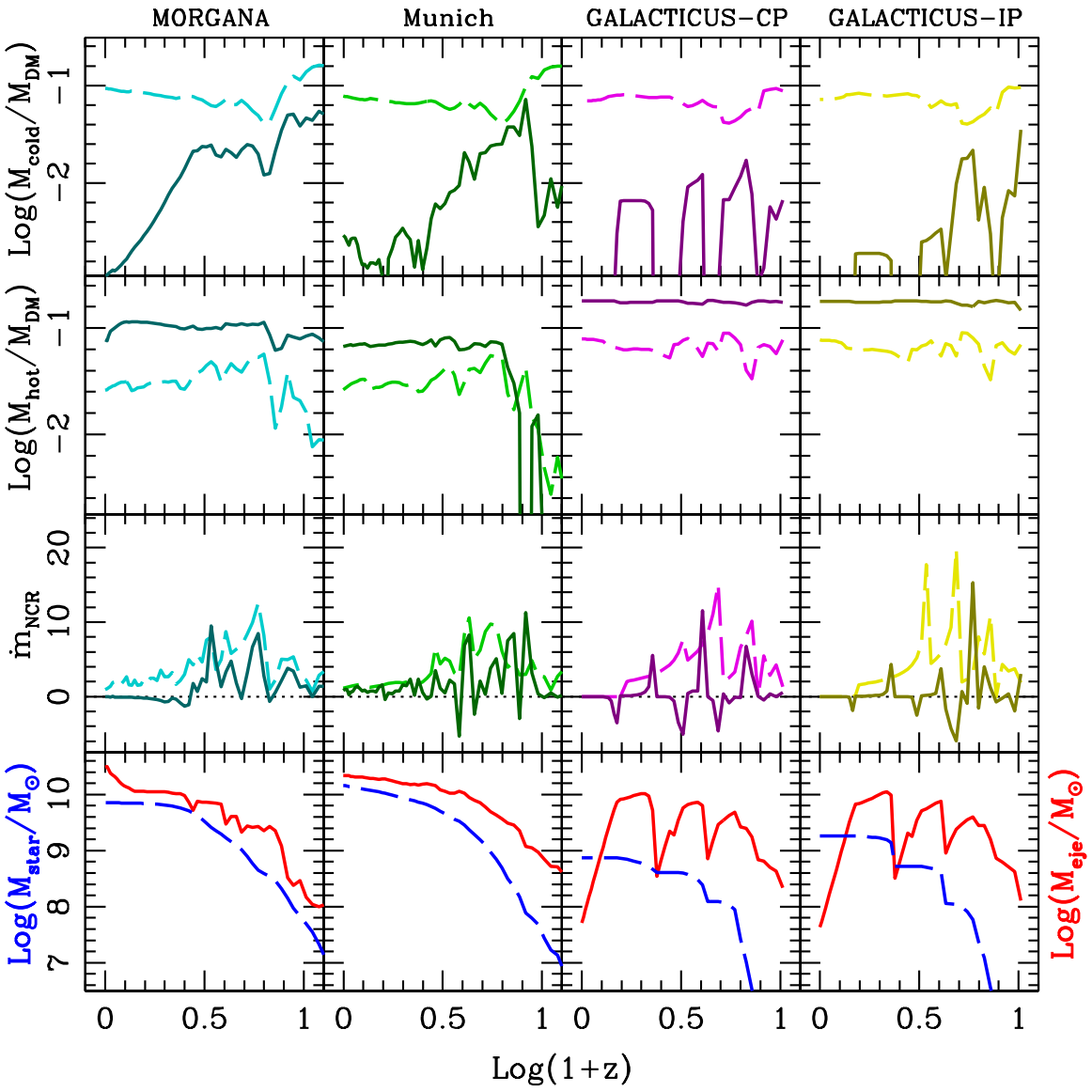

Figure 1: Redshift evolution of the baryonic content for a MW-like representative DMH (with quiet mass accretion history; fig.1 right panels in De Lucia et al. 2010). *Upper row*: cold gas fractions associated with the central galaxy; *second row*: hot gas fractions; *third row*: net cooling rates. Blue, red, yellow and green lines refer to MORGANA , GALACTICUS-CP , GALACTICUS-IP and the *Munich* model. Dark solid lines refer to the models considered in this work, while dashed lines refer to the "cooling only" models (De Lucia et al., 2010). *Lower row*: stellar masses (blue dashed lines) and ejected masses (red solid lines). In all models we assume $t_{\rm mrg} = \infty$ (see text for more details).

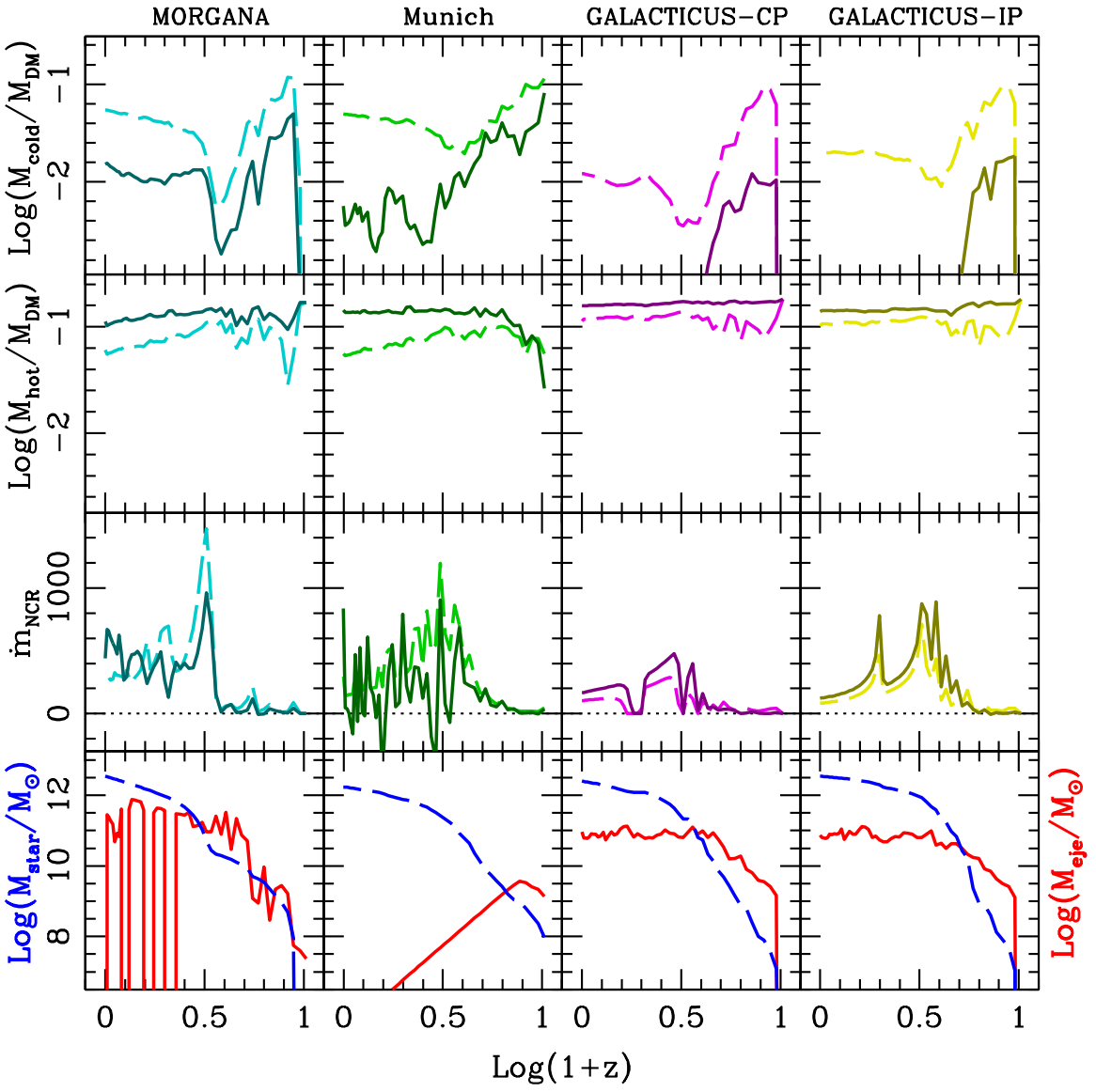

Figure 2: Redshift evolution of the baryonic content for a SCUBA-like representative DMH (with quiet mass accretion history; fig.4 right panels in De Lucia et al. 2010). Symbols, line styles, and colours have the same meaning as in fig. 1.

lar feedback is the main driver of the different evolution of the baryonic components for the models considered in this study.

The combined effect of the decreased cold gas and increased hot component is shown in the third row. In general, the evolution of $\dot{m}_{\rm NCR}$ is not smooth and characterized by epochs of *negative* contribution, i.e. time intervals dominated by outflows able to reduce the cold gas content of the central object. For the MW-like haloes, the evolution of $\dot{m}_{\rm NCR}$ show large deviations from the "cooling-only" configuration, with extended redshift ranges characterized by low or negative rates. This is particularly evident for the *Durham*-like realizations, while the *Munich* model gives predictions that are closest to the cooling rates obtained in the "cooling only" runs.

In the lower panels of fig. 1, we show the redshift evolution of the baryonic mass ejected from the DMH (red solid line) and the stellar mass associated with the central galaxy (blue dashed line). The first quantity is crucial to keep track of the total amount of baryons in each main progenitor, and gives important hints on the impact of stellar feedback. At this mass scale, the ejected component dominates over the stellar mass deposited in the central galaxy for MW-like haloes, (see also De Lucia et al., 2004). We stress that the ejected mass in the *Durham*-like realizations is comparable to the results for the other two models for the MW-like haloes, confirming that the differences in the cold and hot gas fractions are mainly due to the different feedback efficiency and not to an enhanced fraction of material excluded from the mass/energy flows. Indeed, the similar amounts of ejected mass in *Durham*-like and *Munich* models in the whole redshift range, despite $\eta_{\rm rei}^{\rm dur} \gg \eta_{\rm rei}^{\rm mun}$, confirms that the stellar feedback scheme adopted in *Durham*-like models removes a larger fraction of gas from the baryonic budget of these haloes with respect to the *Munich* scheme.

In the same panel we also show the evolution of the central galaxy stellar mass: at this mass scale and with the inclusion of only star formation and stellar feedback, model results are very different. The *Munich* model predicts the largest stellar masses at all redshifts, MORGANA gives slightly lower values for the stellar mass, and both *Durham*-like runs predict stellar masses almost one order of magnitude smaller than the other two models. The GALACTICUS-IP model predicts slightly larger stellar masses with respect to the *Durham*-like models. These results for the *Durham*-like models are consistent with our analysis of the net cooling rate, and are due to a feedback-driven starvation of the cold gas reservoir of the central galaxy. We checked that these conclusions also hold for the redshift evolution of the mean stellar mass in the central galaxy (averaged over the 100 realizations in each DMH sample).

Similar conclusions are reached when considering the representative SCUBA halo (figure 2), but with some significant differences. For these haloes, both the increase of hot gas fraction and the decrease of the cold gas fraction with respect to the "cooling only" versions are less marked, and the prediction of different models are somewhat closer. This is due to the fact that stellar feedback is more efficient in affecting the thermal state of the gas and galaxy evolution on a MW-like scale than in more massive haloes. Consistently, in SCUBA-like haloes $\dot{m}_{\rm NCR}$ follows much more closely the evolution of cooling rates in DL10, and the outflow dominated periods are less frequent or completely absent. As already noticed in DL10, net cooling rates can takes up values of several hundreds of $\rm M_\odot\ yr^{-1}$ with the exception of the GALACTICUS-CP model, where spikes are much less pronounced.

At these mass scales, the ejected component does not dominate over the stellar mass for the SCUBA-like sample (De Lucia et al., 2004) at $z < 2$, and the different feedback models predict a rather different evolution: in the *Durham*-like runs the amount of material in the ejected component stays constant below $z \sim 3$, a more noisy evolution is seen for MORGANA , while in the *Munich* model the ejected mass decreases rapidly and is negligible for the baryonic budget of the haloes at present. The differences in the predictions of the three models are due to the different interplay between the ejected and reincorporated fraction, and again shows that in *Durham*-like models the fraction of ejected material is larger than in the *Munich* model, leading to an almost constant ejected mass, despite the faster reincorporation rate.

Finally, the stellar masses predicted by the three SAMs for the SCUBA-like sample are much closer than in the MW-like sample, with only GALACTICUS-IP predicting slightly higher stellar masses. We interpret also this result as an effect of a less efficient stellar feedback in SCUBA-like haloes for *Durham*-like models: in these models gas cooling is always dominating over cold gas removal (third row) and more material for star formation is available.

Therefore, in this case the marked decrease of the cold gas fraction associated with the central galaxy is the effect of a more efficient star formation.

3.2 Star Formation Histories

We now turn our attention to the stellar mass assembly of the central galaxy as predicted by our SAMs. In figure 3, we consider the evolution, averaged over the whole sample of 100 halos, of the stellar mass in the central galaxies between two contiguous snapshots: in our reference models, with no galaxy mergers, this corresponds to the mean SFR in the object between the two snapshots (dark lines). In order to quantify the relative contribution of the "starburst" mode to central galaxy mass assembly, we also consider the predictions of the instantaneous merger run ($t_{\rm mrg} = 0$) and proceed as follows. We first compute the mean stellar mass variation for central galaxies in the runs with instantaneous mergers: these quantities include both the SFRs in central galaxies and the contribution from satellite mergers. In the no-merger runs, we then consider the mean stellar mass content in satellites already accreted by the main progenitor at each redshift. We then subtract this from the mean stellar mass variations for central galaxies in instantaneous merger runs. This quantity (shown as light lines in the figure) does not strictly correspond to the SFR in the central galaxy in the instantaneous merger runs, since enhanced SFR episodes in satellites are not properly subtracted. Clearly, the instantaneous merger runs correspond to an extreme case, since in a realistic SAM run only a fraction of satellites is allowed to merge onto their central galaxy. Nonetheless, the comparison of dark and light line provides a conservative upper limit to the overall starburst mode contribution to the assembly of the central object.

In each panel of figure 3, we consider the mean variation of stellar mass in the two different sets of runs, averaged over the 100 MW-like (upper panels) and SCUBA-like haloes (lower panels). In the left panels, we directly compare the no merger runs with the instantaneous merger runs modified as described above for each SAM, to show the contribution of the starburst mode in each configuration. In the right panels, we compare the different predictions of our SAMs in the same runs.

Let us focus first on the MW-like sample. As far as the no merger runs are considered, MORGANA and the *Munich* model predictions are very close to each other at early times, and start diverging at lower redshifts, with MORGANA predicting less star formation than the *Munich* model. At the same mass scales, the GALACTICUS realizations show lower SFRs at all redshifts. With respect to the *Munich* model, the difference is about one order of magnitude, while at lower redshifts the difference with MORGANA predictions is reduced. The GALACTICUS-IP predicts systematically higher SFRs at all redshift than the GALACTICUS-CP run. These results are consistent with our findings in sec. 3.1, and are directly related to the differences in net cooling rates among the SAMs. We compare these results with the analogous prediction for the instantaneous merger runs, thus showing the maximum expected contribution from the starburst mode of star formation. In general the overall growth rate of the central galaxy is enhanced in all SAMs. The largest contributions are seen at low redshift for MORGANA (at $z < 3$, reaching a factor of 8 at $z \sim 0$) and for GALACTICUS-IP (a factor of 4 at $z < 1$), while the *Munich* model shows a smaller (at most a factor of 2) increase at all redshift. The smallest modifications are seen for GALACTICUS-CP (only a few percent).

We then focus the SCUBA-like sample. For the no merger runs, the predictions of the different models are generally closer than for the MW-like sample. At these mass scales, the predictions of the different GALACTICUS realizations are more similar to those from the *Munich* model and MORGANA , and they show higher SFRs at earlier times ($z \gtrsim 2$). Again, GALACTICUS-IP realizations predicts systematically higher SFRs with respect to GALACTICUS-CP realizations. Also for this sample, the instantaneous merger runs predict an enhancement of the stellar mass formed, but in this case the variations are well below a factor of two in all cases, with the maximum deviation seen for MORGANA at intermediate ($z \sim 3$) redshifts (it is worth recalling that the two examples of figures 2 and 7 show spiky deposition rates for three out of four models; these differences are not visible in the SFR when it is averaged over 100 halos). These results shows that, at these mass scales, the impact of merger-driven starburst is limited. This is in line with the phenomenological estimate of Sargent et al. (2012) of an 8-14 per cent contribution of mergers to the total SFR.

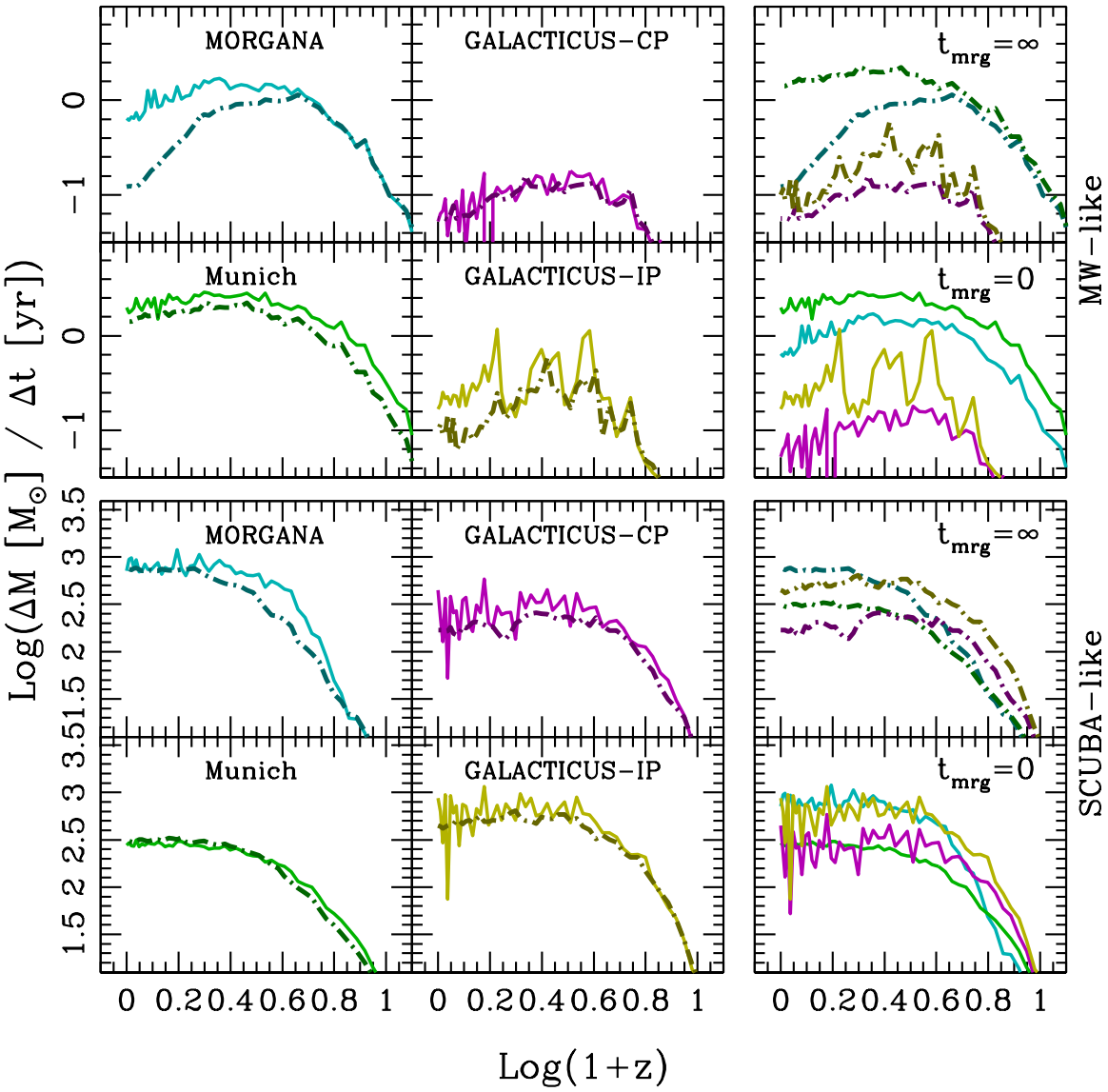

Figure 3: Average evolution of central galaxy stellar mass as a function of redshift (over 100 DMHs - see text for more details). Blue, red, yellow and green lines refer to MORGANA , GALACTICUS-CP , GALACTICUS-IP and the *Munich* model. Dark dot-dashed lines refer to the $t_{\rm mrg} = \infty$ realizations, while light solid lines correspond to the instantaneous merger runs. Upper panels refer to the MW-like sample, while lower panels to the SCUBA-like sample. Left panels compare the no merger and the instantaneous merger runs for each SAM separately, while right panels compare the average prediction of different SAMs in the same configuration.

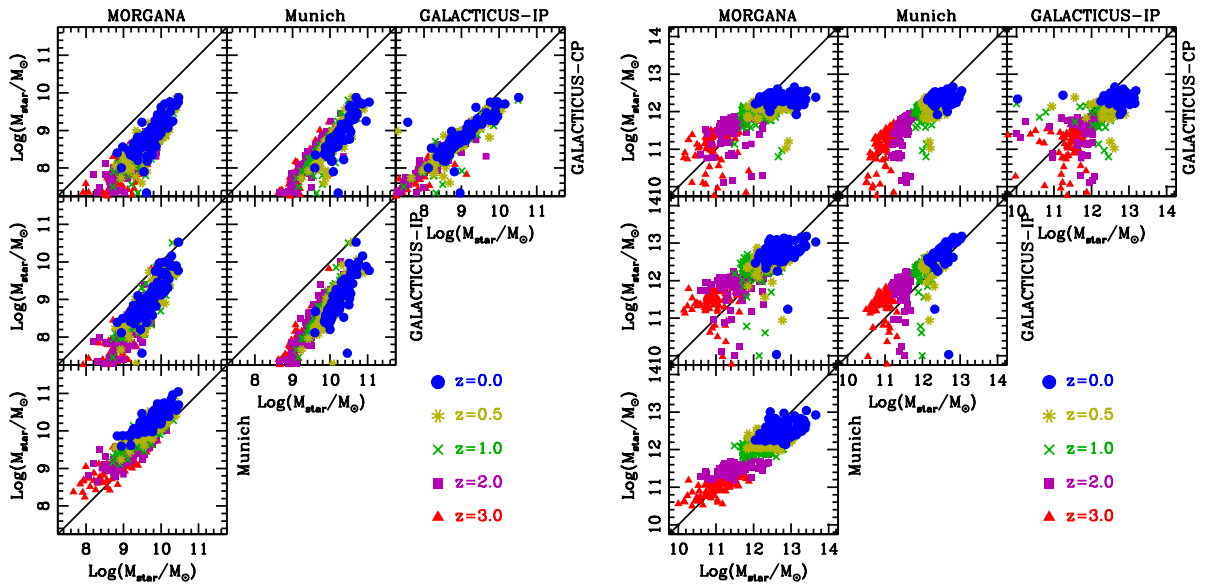

Figure 4: Comparison of central galaxy stellar masses for the 100 MW-like (*left panel*) and SCUBA-like(*right panel*) haloes. In each panel, blue circles, yellow asterisks, green crosses, purple squares and red triangles refer to model predictions at $z = [0; 0.5; 1; 2; 3]$ respectively.

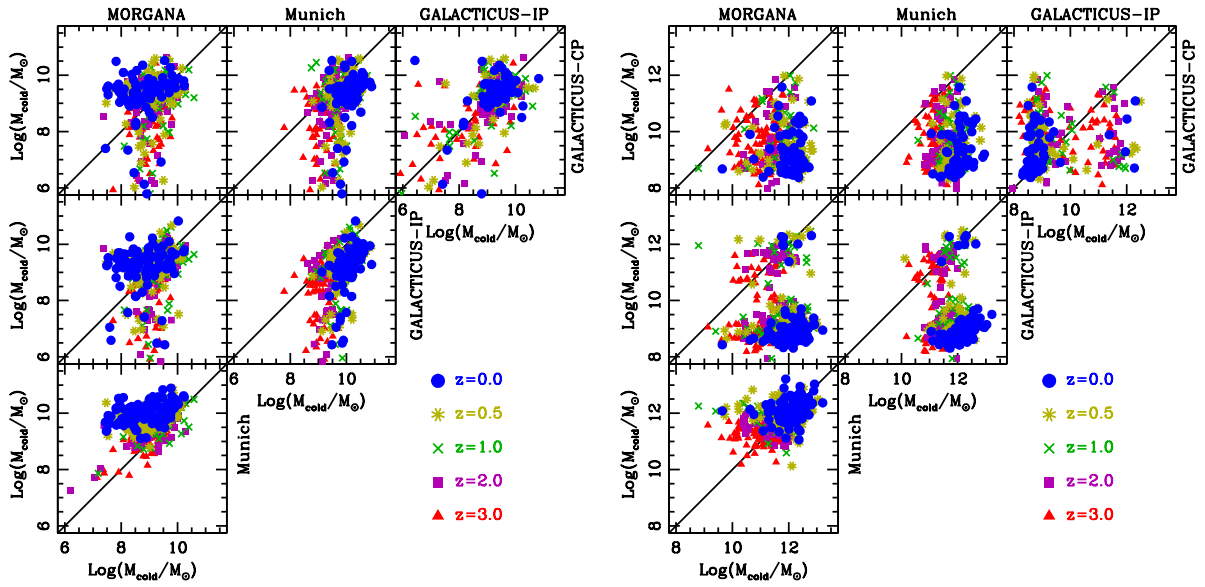

Figure 5: Same as fig. 4 for cold gas masses associated with the central galaxy in the 100 MW-like (*left panel*) and SCUBA-like(*right panel*) haloes. Symbols and colours are the same as in fig. 4.

3.3 Stellar and gas content at different redshifts

In order to get more insight into the mass assembly process predicted by our models, we compare in fig. 4 the model stellar masses for the central galaxy at different redshift on an object-by-object basis. Left and right panels refer to the MW-like and SCUBA-like haloes, respectively. Each pair of models show some degree of correlation in the predicted stellar masses, and this confirms the overall consistency of the models. For the MW-like haloes, the stellar content predicted by the *Durham*-like realizations is offset low with respect to predictions from the other models. Moreover, the overall slope of the relation looks steeper than the one-to-one correlation, with smaller galaxies deviating more from the one-to-one relation. This shows that the difference is due to the mass depencence of the efficiency of feedback in regulating star formation. For the SCUBA-like haloes, the stellar masses predicted from the three models considered are very close. GALACTICUS-CP is the only model deviating considerably from the one-to-one relation, particularly at low redshift, reflecting the fact that these galaxies grow more slowly in the GALACTICUS-CP realizations than in MORGANA or the *Munich* model. We also consider the corresponding predictions for the "instantaneous merger" run (not shown in the figure): we find that all central galaxies in SCUBA-like haloes at all redshift lie along the one-to-one line, while our conclusions are qualitatively unchanged in MW-like haloes. For these runs, the scatter in the correlations is reduced in both samples at all redshift: we thus conclude that the presence of mergers helps the predictions of the models to converge to a common value, and this effect gets stronger with increasing number of mergers.

We also consider the corresponding cold gas content associated with the central galaxy on an object-by-object basis (fig. 5). The differences between the SAMs are even more evident for this physical quantity in both samples. MORGANA and the *Munich* model show the strongest correlation both for the MW-like and SCUBA-like haloes, while the *Durham*-like realizations show no correlation at all with the predictions of the other two models. It is worth stressing that in SCUBA-like haloes *Durham*-like realizations predict cold gas amounts $1-2$ orders of magnitude lower than the corresponding MORGANA and *Munich* predictions. The results are similar between GALACTICUS-CP and GALACTICUS-IP , implying that this depletion is not only related to the smaller cooling flows associated with the cored-profile, but that stellar feedback is also playing an important role in removing cold gas content from the haloes. However, it is not possible to indicate stellar feedback as the only responsible for the smaller stellar masses obtained in MW-like haloes. Indeed, the cold gas content of these haloes in the *Durham*-like runs may be even larger than the corresponding MORGANA and *Munich* predictions. Therefore, it is the interplay between star formation and feedback that is responsible for the different predictions.

4 Discussion & Conclusions

We compared predictions of three independently developed semi-analytic models of galaxy formation, focusing our analysis on their assumed modelling for the physical processes involving star formation and stellar feedback. Following the same approach as in De Lucia et al. (2010, DL10) we define "stripped down" SAM versions including cooling, star formation, feedback from supernovae (SNe) and simplified prescriptions for galaxy merging, and we run them on the same samples of DMH merger trees, extracted from the Millennium and Millennium-II Simulations.

The choice of "stripped-down" versions of the SAMs has the advantage of avoiding complications due to other processes like disc instabilities, metal enrichment and AGN feedback. In our "stripped-down" versions we either assume $t_{\rm mrg} = \infty$ or $t_{\rm mrg} = 0$, in order to remove the additional degeneracies due to different definitions of merging times (see DL10). Our aim is to discuss the influence of specific model ingredients on the physical properties of model galaxies. In the following, we summarise and discuss our main findings.

- *Supernovae feedback:* As expected, switching on star formation and stellar feedback has important consequences on the different gas phases in DMHs, with respect to the "cooling only" SAM versions: the amount of cold gas available is reduced, while the hot gas fraction is increased. While we find an encouraging level of consistency between the mod-

els, the specific star formation and SN feedback prescriptions in each model induce differences in the stellar and gaseous content of galaxies. This is in line with what is found in numerical simulations of MW-like galaxies performed with different codes (Scannapieco et al., 2012). In particular, we find that the scheme adopted by the *Durham*-like models provides larger hot gas fractions with respect to the other two models and a rapid depletion of the cold gas fraction in galaxies. The amount of gas that is in an 'ejected' component (i.e. temporarily not associated with the halo/galaxy) is similar in the three models considered, though its redshift evolution can differ significantly.

- *Stellar content:* If we consider the average SFRs in the MW-like sample, MORGANA and the *Munich* model predictions show a good level of agreement at $z \gtrsim 2$: predictions from the two models deviate at later times, which has only a limited effect on the predicted $z = 0$ stellar masses. For this sample, the most striking differences are between predictions of MORGANA (or the *Munich* model) and those from the *Durham*-like realizations. In fact, the star formation and feedback schemes implemented following Bower et al. (2006) predict significantly lower SFR levels at all redshifts. As a consequence, the *Durham*-like models predicts systematically lower stellar masses for the corresponding central objects with respect to both MORGANA and the *Munich* model. The discrepancy is a weak function of stellar mass itself, being smaller for more massive galaxies (within a given DMH sample). For SCUBA-like haloes, the differences between the predicted SFRs are smaller than for MW-like haloes, and the predicted stellar masses are much closer at all redshifts, the biggest difference being a more rapid assembly of stellar mass in the central object at earlier times in the *Durham*-like runs.
- *Quiescent and starburst modes of star formation:* We analysed the impact of the "starburst" mode of star formation (usually associated with galaxy mergers) by comparing runs obtained with infinite and vanishing galaxy merging times; this approach allows us to give an upper limit on the contribution of the starburst mode. In most cases we found an increase of the average mass assembly rate of the central galaxy not larger than a factor of 2, with the largest contributions found in the MORGANA model. This shows that the contribution of the starburst mode of star formation in the overall SFR budget is limited, in line with, e.g., Sargent et al. (2012). We also find that the inclusion of merger driven starbursts decrease the scatter in the predicted stellar masses at given redshift between haloes in the same DMH sample.

These results extend and deepen our conclusion presented in DL10 to include the comparison of different approaches to the modeling of star formation and feedback in SAMs. Despite the general coherent picture for the impact of the energy injection connected to stellar feedback on the distribution of baryons into the different gas phases, each feedback model is characterized by its unique pattern in tracing the redshift evolution of the different baryonic components (cold gas, hot gas, ejected gas) and this information is fundamental to understand the building up of galaxy properties in a cosmological context.

Acknowledgements

FF acknowledges financial support from the Klaus Tschira Foundation and the Deutsce Forschungsgemeinschaft through Transregio 33, "The Dark Universe". GDL acknowledges financial support from the European Research Council under the European Community's Seventh Framework Programme (FP7/2007- 2013)/ERC grant agreement n. 202781. MBK acknowledges support from the Southern California Center for Galaxy Evolution, a multi-campus research program funded by the University of California Office of Research. Some of the calculations were carried out on the "Magny" cluster of the Heidelberger Institute für Theoretische Studien. The Millennium and Millennium-II Simulation data bases and the web application providing online access to them were constructed as part of the activities of the German Astrophysical Virtual Observatory. We are grateful to Gerard Lemson for setting up an internal data base that greatly facilitated the exchange of data and information needed to carry out this project.

References

Baugh C. M., 2006, Reports of Progress in Physics, 69, 3101

Benson A. J., 2012, NewA, 17, 175

Benson A. J., Bower R. G., Frenk C. S., Lacey C. G., Baugh C. M., Cole S., 2003, ApJ, 599, 38

Bower R. G., Benson A. J., Malbon R., Helly J. C., Frenk C. S., Baugh C. M., Cole S., Lacey C. G., 2006, MNRAS, 370, 645

Boylan-Kolchin M., Springel V., White S. D. M., Jenkins A., Lemson G., 2009, MNRAS, 398, 1150

Chapman S. C., Smail I., Windhorst R., Muxlow T., Ivison R. J., 2004, ApJ, 611, 732

Cole S., Lacey C. G., Baugh C. M., Frenk C. S., 2000, MNRAS, 319, 168

Cox T. J., Primack J., Jonsson P., Somerville R. S., 2004, ApJ, 607, L87

Croton D. J., Springel V., White S. D. M., De Lucia G., Frenk C. S., Gao L., Jenkins A., Kauffmann G., Navarro J. F., Yoshida N., 2006, MNRAS, 365, 11

De Lucia G., Blaizot J., 2007, MNRAS, 375, 2

De Lucia G., Boylan-Kolchin M., Benson A. J., Fontanot F., Monaco P., 2010, MNRAS, 406, 1533

De Lucia G., Fontanot F., Wilman D., Monaco P., 2011, MNRAS, 414, 1439

De Lucia G., Kauffmann G., White S. D. M., 2004, MNRAS, 349, 1101

Fontanot F., De Lucia G., Monaco P., Somerville R. S., Santini P., 2009, MNRAS, 397, 1776

Fontanot F., De Lucia G., Wilman D., Monaco P., 2011, MNRAS, 416, 409

Fontanot F., Pasquali A., De Lucia G., van den Bosch F. C., Somerville R. S., Kang X., 2011, MNRAS, 413, 957

Kauffmann G., 1996, MNRAS, 281, 487

Lo Faro B., Monaco P., Vanzella E., Fontanot F., Silva L., Cristiani S., 2009, MNRAS, 399, 827

Mo H. J., Mao S., White S. D. M., 1998, MNRAS, 295, 319

Monaco P., 2004, MNRAS, 352, 181

Monaco P., Fontanot F., Taffoni G., 2007, MNRAS, 375, 1189

Sargent M. T., Béthermin M., Daddi E., Elbaz D., 2012, ApJ, 747, L31

Scannapieco C., Wadepuhl M., Parry O. H., Navarro J. F., Jenkins A., Springel V., Teyssier R., Carlson e. a., 2012, MNRAS, 423, 1726

Somerville R. S., Primack J. R., Faber S. M., 2001, MNRAS, 320, 504

Springel V., White S. D. M., Jenkins A., Frenk C. S., Yoshida N., Gao L., Navarro J., Thacker R., Croton D., Helly J., Peacock J. A., Cole S., Thomas P., Couchman H., Evrard A., Colberg J., Pearce F., 2005, Nature, 435, 629

Springel V., White S. D. M., Tormen G., Kauffmann G., 2001, MNRAS, 328, 726

A Predictions for representative haloes with merger-dominated mass accretion histories.

For consistency with DL10, we show in this appendix the two DMHs chosen among the 100 scuba-like and the 100 MW-like as representatives of haloes with a significant number of merger events along their assembly history (compare with results in sec. 3.1).

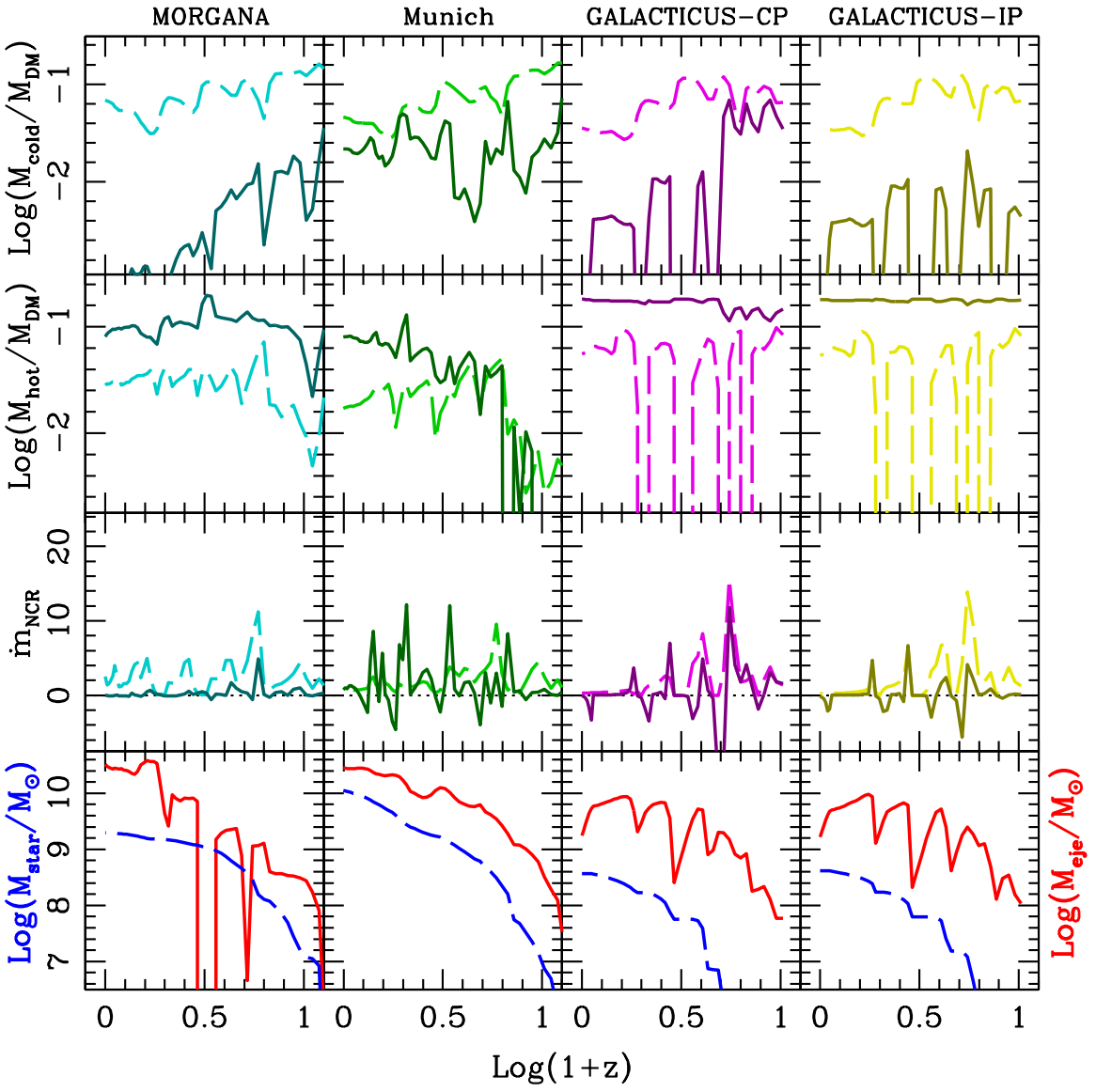

Figure 6: Redshift evolution of the baryonic content of a MW-like representative DMH (with merger-dominated mass accretion history; fig.1 left panels in De Lucia et al. 2010). Symbols, line styles, and colours are as in fig. 1.

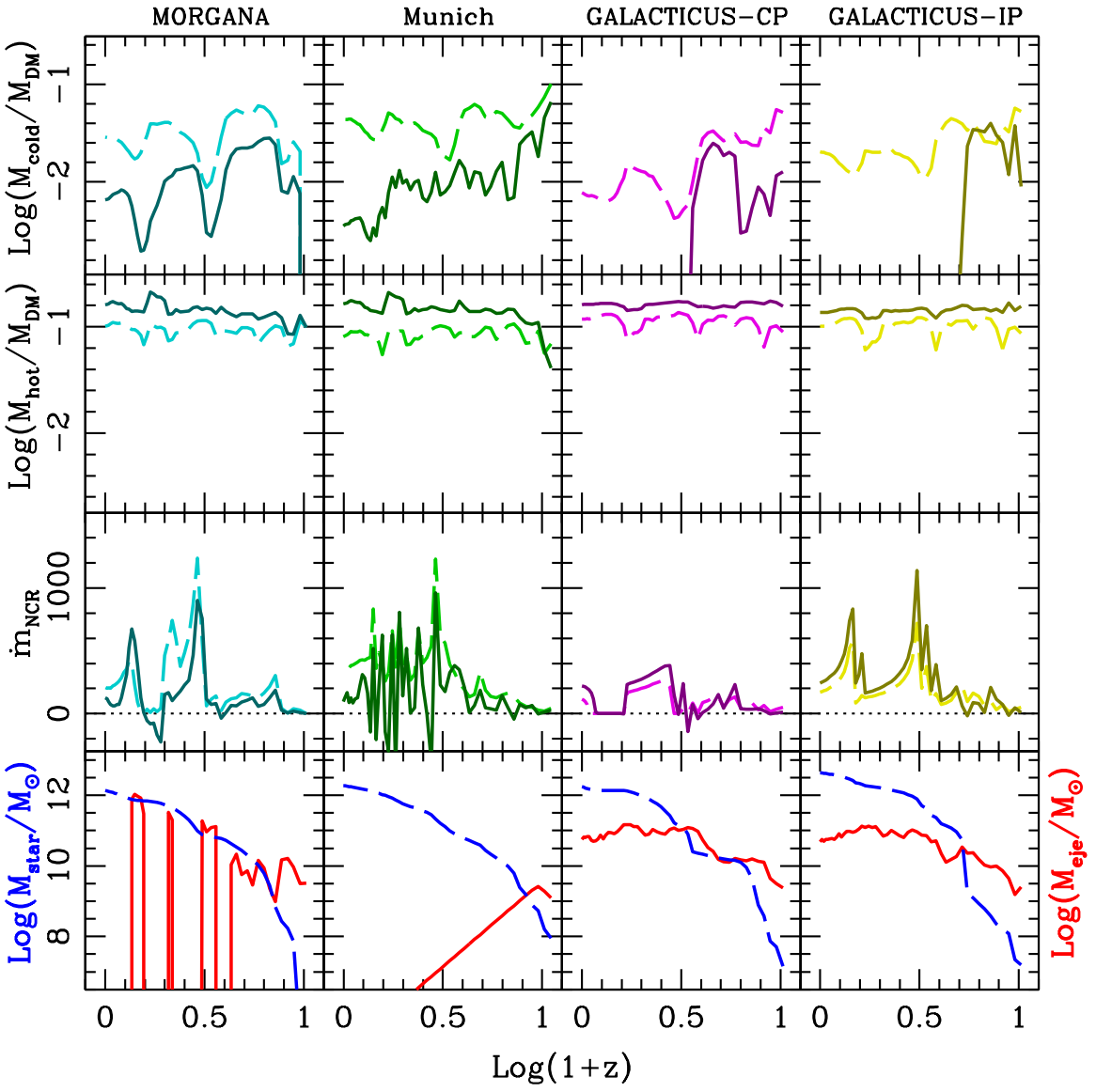

Figure 7: Redshift evolution of the baryonic content of a SCUBA-like representative DMH (with merger-dominated mass accretion history; fig.4 left panels in De Lucia et al. 2010). Symbols, line styles, and colours are as in fig. 1.